Matrix Isolation Infrared Spectroscopic Studies and Density Functional Theory Calculations of the MNN, $(MN)_2$ (M = Y and La), and Y_3NN Molecules

Yun-Lei Teng and Qiang Xu*

National Institute of Advanced Industrial Science and Technology, Ikeda, Osaka 563-8577, Japan, and Graduate School of Engineering, Kobe University, Nada Ku, Kobe, Hyogo 657-8501, Japan

Received: November 15, 2007; In Final Form: January 28, 2008

The reactions of yttrium and lanthanum with dinitrogen were reinvestigated. Laser-ablated yttrium and lanthanum atoms were co-deposited at 4 K with dinitrogen in excess argon, and the low-temperature reactions of Y and La with N_2 in solid argon were studied using infrared spectroscopy. The reaction products YNN, $(YN)_2$, LaNN, and $(LaN)_2$ were formed in the present experiments and characterized on the basis of $^{14}N/^{15}N$ isotopic shifts, mixed isotope splitting patterns, stepwise annealing, change of reagent concentration and laser energy, and comparison with theoretical predictions. Some assignments were made based on a previous report. Density functional theory calculations were performed on these systems to identify possible reaction products. The agreement between experimental and calculated vibrational frequencies, relative absorption intensities, and isotopic shifts of the MNN and $(MN)_2$ (M = Y and La) molecules supports the identification of these molecules from the matrix infrared spectra. Plausible reaction mechanisms were proposed for the formation of these molecules along with tentative identification of the Y_3NN molecule.

Introduction

The bonding of dinitrogen with transition metals is of great interest from both academic and industrial viewpoints because the binding of dinitrogen to transition metal centers may lead to the cleavage of the strong N−N bond as in the catalytic synthesis of ammonia.[1−3] The long-standing goal of elucidating mechanisms of the reactions involving dinitrogen has motivated numerous experimental and theoretical investigations of the interactions between metals and dinitrogen.[4−11] Complexes, such as ScNN, $Sc(N_2)$, ScN, and $(ScN)_2$, were produced and characterized using matrix isolation infrared spectroscopy.[11c] The reactions of laser-ablated yttrium and lanthanum with dinitrogen also have been studied. The complicated IR spectra in the previous experiment with a high concentration of N_2 were attributed to $M(N_2)$ and $(MN)_2$ (M = Y and La) along with a number of Y and La nitrides and dinitrogen complexes, among which some species were tentatively assigned.[11a]

Recent studies have shown that, with the aid of isotopic substitution techniques, matrix isolation infrared spectroscopy combined with quantum chemical calculations is very powerful for investigating the structure and bonding of novel species.[12] To further understand the formations of nitrides and dinitrogen species of yttrium and lanthanum, the reactions of laser-ablated yttrium and lanthanum atoms with N_2 in a solid argon matrix were performed. IR spectroscopy and theoretical calculations provide evidence for the formation of products, such as YNN, $(YN)_2$, Y_3NN, LaNN, and $(LaN)_2$. As compared to the previous report on the reactions of Y and La atoms with a high concentration of dinitrogen without theoretical calculations,[11a] the present work on the reactions of Y and La with a low concentration of N_2 produced simplified IR spectra, with which we find a new tentative product Y_3NN, make more definitive assignments for the YNN and LaNN molecules, and characterize the $(YN)_2$ and $(LaN)_2$ molecules in more detail with isotopic investigations and DFT calculations.

Experimental and Theoretical Methods

The experiments for laser ablation and matrix isolation infrared spectroscopy are similar to those previously reported.[13] Briefly, the Nd:YAG laser fundamental (1064 nm and 10 Hz repetition rate with 10 ns pulse width) was focused on the rotating Y and La targets. The laser-ablated species were co-deposited with N_2 (99.95%) in excess argon onto a CsI window cooled normally to 4 K by means of a closed-cycle helium refrigerator (V24SC6LSCP, Daikin Industries). Typically, a 5−15 mJ/pulse laser power was used. Isotopic substituted $^{15}N_2$ (99.8%) and $^{14}N_2 + {}^{15}N_2$ and high-frequency discharging scrambled $^{14}N_2 + 2^{14}N^{15}N + {}^{15}N_2$ mixtures were used in different experiments. In general, matrix samples were deposited for 30−60 min with a typical rate of 2−4 mmol h^{-1}. After sample deposition, IR spectra were recorded on a Bio-Rad FTS-6000e spectrometer at 0.5 cm^{-1} resolution using a liquid nitrogen cooled HgCdTe (MCT) detector for the spectral range of 5000−400 cm^{-1}. Samples were annealed at different temperatures and subjected to broad-band irradiation ($\lambda > 250$ nm) using a high-pressure mercury arc lamp (Ushio, 100 W).

Quantum chemical calculations were performed to predict the structures and vibrational frequencies of the observed reaction products using the Gaussian 03 program.[14] The BP86 and B3LYP density functional methods were utilized.[15] The 6-311++G(d,p) basis set was used for N atoms, and SDD was used for Y and La atoms.[16,17] Geometries were fully optimized, and vibrational frequencies were calculated with analytical second derivatives.

Results and Discussion

Experiments were performed with N_2 concentrations ranging from 0.02 to 0.2% in excess argon. Typical infrared spectra for

* Author to whom correspondence should be addressed. E-mail: q.xu@aist.go.jp.

10.1021/jp8003568 CCC: $40.75
Published on Web 03/18/2008

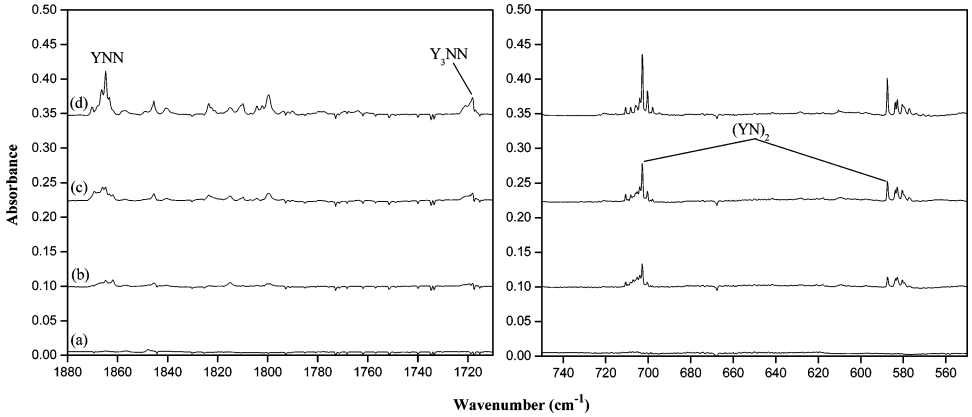

Figure 1. Infrared spectra in the 1880−1710 and 750−550 cm^{-1} regions from co-deposition of laser-ablated Y atoms with 0.05% N_2 and 15 mJ/pulse laser power in argon: (a) 60 min sample deposition at 4 K; (b) after annealing to 25 K; (c) after annealing to 30 K; and (d) after annealing to 35 K.

TABLE 1: Infrared Absorptions (cm^{-1}) from Co-deposition of Laser-Ablated Y and La Atoms with N_2 in Excess Argon at 4 K

$^{14}N_2$	$^{15}N_2$	$^{14}N_2 + {}^{15}N_2$	$^{14}N_2 + {}^{14}N^{15}N + {}^{15}N_2$	$^{14}N/^{15}N$	assignment (mode)[a]
1864.7	1802.6	1864.7, 1802.6	1864.7, 1835.2, 1832.7, 1802.7	1.0345	YNN N−N str.
1845.5	1783.5			1.0348	$(NN)_xY(N_2)$ N−N str.
1823.4	1762.8			1.0344	$(NN)_xY(N_2)$ N−N str.
1799.6	1741.6			1.0333	$(NN)_xY(N_2)$ N−N str.
1718.1	1662.0	1718.3, 1662.0	1718.0, 1690.7, 1687.1, 1662.3	1.0338	Y_3NN N−N str.
702.8	682.6	702.8, 682.6	702.8, 692.9, 682.6	1.0296	$(YN)_2$ Y−N str.
587.5	570.4	587.4, 570.5	587.5, 577.6, 570.6	1.0300	$(YN)_2$ Y−N str.
1826.4	1765.9			1.0343	$(NN)_x$ LaNN N−N str.
1797.0	1737.4			1.0343	$(NN)_x$ LaNN N−N str.
1791.6	1732.3			1.0342	$(NN)_x$ LaNN N−N str.
1749.8	1692.2	1749.9, 1692.3	1749.7, 1723.1, 1719.2, 1692.2	1.0340	LaNN N−N str.
652.6	632.9	652.6, 632.8	652.6, 642.9, 632.9	1.0311	$(LaN)_2$ La−N str.
530.1	513.9	530.1, 514.0	530.1, 521.1, 513.9	1.0315	$(LaN)_2$ La−N str.

[a] str. is stretching mode.

TABLE 2: Comparison of Observed and Calculated IR Frequencies (cm^{-1}) and Isotopic Frequency Ratios of Reaction Products

		exptl		calcd		
molecule	mode[a]	freq.[a]	$^{14}N/^{15}N$	method	freq.[a]	$^{14}N/^{15}N$
YNN	N−N str.	1864.7	1.0345	BP86	1814.7	1.0350
				B3LYP	1853.6	1.0350
$(YN)_2$	Y−N str. (b_{1u})	702.8	1.0296	BP86	711.2	1.0300
				B3LYP	726.2	1.0299
	Y−N str. (b_{2u})	587.5	1.0300	BP86	557.7	1.0301
				B3LYP	569.9	1.0300
Y_3NN	N−N str.	1718.1	1.0338	BP86	1684.4	1.0350
				B3LYP	1743.3	1.0350
LaNN	N−N str.	1749.8	1.0340	BP86	1762.4	1.0350
				B3LYP	1834.5	1.0350
$(LaN)_2$	La−N str. (b_{1u})	652.6	1.0311	BP86	668.9	1.0316
				B3LYP	677.8	1.0317
	La−N str. (b_{2u})	530.1	1.0315	BP86	532.0	1.0316
				B3LYP	540.5	1.0317

[a] str. is stretching mode and freq. is frequency.

the reactions of laser-ablated Y and La with N_2 in excess argon in the selected regions are illustrated in Figures 1−6, and the absorption bands are listed in Table 1. The stepwise annealing and broad-band irradiation behavior of these product absorptions also are shown in Figures 1−6.

Quantum chemical calculations were carried out for the possible isomers and electronic states of the potential product molecules. Figure 7 shows the optimized structures and electronic ground states. Table 2 reports a comparison of the observed and calculated IR frequencies and isotopic frequency ratios of the reaction products. Calculated vibrational frequencies and intensities of the potential products are listed in Table 3.

YNN. For the experiments of laser-ablated Y atoms with N_2, the absorption at 1864.7 cm^{-1} with two trapping sites at 1870.1 and 1866.3 cm^{-1} appears on annealing to 25 K, visibly increases on annealing to 30 K, and markedly increases on annealing to 35 K (Figure 1). It shifts to 1802.6 cm^{-1} with $^{15}N_2$, giving an isotopic $^{14}N/^{15}N$ ratio of 1.0345, which is characteristic of a N−N stretching vibration. No intermediate absorptions are observed in the mixed $^{14}N_2 + {}^{15}N_2$ experiments, indicating that only one N_2 subunit is involved in this mode (Figure 3). In the experiment with 0.05% $^{14}N_2$ + 0.1% $^{14}N^{15}N$ + 0.05% $^{15}N_2$, four absorptions at 1864.7, 1835.2, 1832.7, and 1802.7 cm^{-1} with approximately 1:1:1:1 relative intensities are produced (Figure 3), which implies that the two N atoms are nonequivalent. Doping with CCl_4 has no effect on the band, which suggests that the product is neutral. Accordingly, this band is assigned to the N−N stretching vibration of the neutral YNN complex, which is in agreement with the previous tentative assignment in solid argon (1864.1 cm^{-1}).[11a]

BP86 calculations predict YNN to have a $^4\Sigma^+$ ground state with a linear geometry, which lies 3.0 kcal/mol lower in energy than the Y(η^2-N_2) isomer (Figure 7). The N−N stretching vibrational frequency of YNN is calculated at 1814.7 cm^{-1} (Tables 2 and 3), which is in accord with our observed value. As listed in Table 2, the calculated $^{14}N/^{15}N$ isotopic frequency ratio (1.0350) also is consistent with the experimental observation (1.0345). B3LYP calculations give results consistent with the BP86 calculations (Table 2). The assignment of the YNN molecule is supported by the agreement between the experimental and the calculated vibrational frequencies and isotopic shifts.

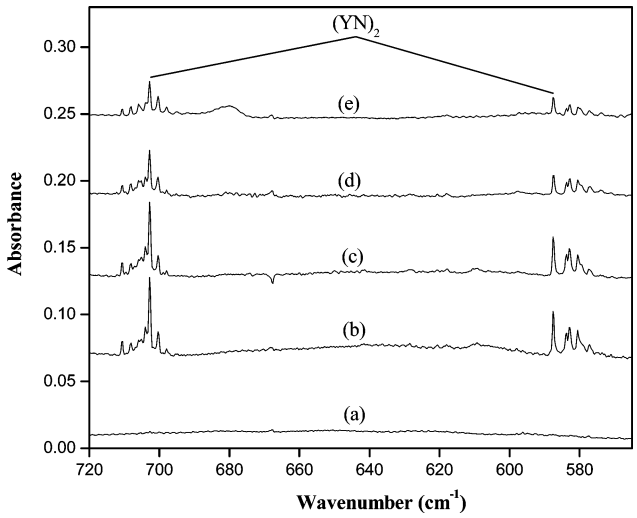

Figure 2. Infrared spectra in the 720−560 cm^{-1} region from co-deposition of laser-ablated Y atoms with different N_2 concentrations and different laser powers after annealing to 30 K in argon: (a) 0.05% N_2 and 5 mJ/pulse; (b) 0.05% N_2 and 8 mJ/pulse; (c) 0.05% N_2 and 15 mJ/pulse; (d) 0.2% N_2 and 15 mJ/pulse; and (e) 0.5% N_2 and 15 mJ/pulse.

$(YN)_2$. For the experiments of laser-ablated Y atoms with N_2, the absorptions at 702.8 and 587.5 cm^{-1} appear on samples annealing to 25 K and markedly increase on annealing to 30 and 35 K (Figure 1). The two bands, respectively, shift to 682.6 and 570.4 cm^{-1} with $^{15}N_2$, giving isotopic frequency ratios ($^{14}N/^{15}N$, 1.0296 and 1.0300) characteristic of M−N stretching vibrations. No intermediate absorptions are observed in the mixed $^{14}N_2 + {}^{15}N_2$ experiments, indicating that only two N atoms are involved in this mode (Figure 3). In the experiment with 0.05% $^{14}N_2$ + 0.1% $^{14}N^{15}N$ + 0.05% $^{15}N_2$, two sets of triplet bands with approximate 1:2:1 relative intensities (Table 1 and Figure 3) are produced, which indicates that two equivalent N atoms are involved. As shown in Figure 2, in the experiments with different N_2 concentrations and laser powers, the absorptions at 702.8 and 587.5 cm^{-1} appear and exhibit the same annealing behavior. Doping with CCl_4 has no effect on the two bands, which suggests that the product is neutral. The two bands are assigned to the Y−N stretching vibrations of the neutral $(YN)_2$ complex. It is noted that in the previous experiment with a high concentration of N_2, the two bands at 710.4 and 586.9 cm^{-1} were assigned to the $(YN)_2$ molecule.[11a]

For $(YN)_2$, all possible structures were calculated using DFT methods. The $(YN)_2$ molecule is predicted to have a ^1A_g ground state with D_{2h} rhombic geometry (Figure 7), which is 20.0 and 60.5 kcal/mol lower in energy than the triplet and quintet ones, respectively. The rhombic $(MN)_2$ molecules also appear in the reactions of laser-ablated Sc, Co, and Ni atoms with N_2.[11c,e] The present DFT calculations predict that $(YN)_2$ has b_{1u} and b_{2u} Y−N stretching vibrational frequencies at 711.2 and 557.7 cm^{-1} with an intensity ratio of 203:134 (Tables 2 and 3), respectively, which are in accord with our observed frequencies (702.8 and 587.5 cm^{-1}) and intensity ratios. The b_{3u} vibrational frequency is predicted to be 225.5 cm^{-1}, which is in the far-IR region. The present observation is in disagreement with the previous report, in which the two absorptions at 710.4 and 586.9 cm^{-1} were assigned to the b_{2u} and b_{3u} vibrations.[11a] As listed in Table 2, the calculated $^{14}N/^{15}N$ isotopic frequency ratios (1.0300 and 1.0301) also are consistent with the experimental observations (1.0296 and 1.0300). According to our DFT calculations, the b_{3u} mode frequency (225.5 cm^{-1}) of $(YN)_2$ is too low to be observed in the present experiment (Table 3). The assignment of the $(YN)_2$ molecule is supported by the agreement between the experimental and the calculated vibrational frequencies and isotopic shifts.

Y_3NN. For the experiments of laser-ablated Y atoms with N_2, the absorption at 1718.1 cm^{-1} appears on annealing to 25 K, visibly increases on annealing to 30 K, and markedly increases on annealing to 35 K (Figure 1). It shifts to 1662.0 cm^{-1} with $^{15}N_2$, giving an isotopic $^{14}N/^{15}N$ ratio of 1.0338, which is characteristic of a N−N stretching vibration. No intermediate absorptions are observed in the mixed $^{14}N_2 + {}^{15}N_2$ experiments, indicating that only one N_2 subunit is involved in this mode (Figure 3). In the experiment with 0.05% $^{14}N_2$ + 0.1% $^{14}N^{15}N$ + 0.05% $^{15}N_2$, four absorptions at 1718.0, 1690.7, 1687.1, and 1662.3 cm^{-1} with approximately 1:1:1:1 relative intensities are produced (Figure 3), which implies that the two N atoms are inequivalent. Furthermore, this band is favored with a higher laser energy, indicating that more than one Y atom is involved. The 1718.1 cm^{-1} band lies in the region expected for the N−N stretching vibration of bridging dinitrogen species. Doping with CCl_4 has no effect on the band, which suggests that the product is neutral. As described next, our theoretical calculations exclude the formation of a $Y_2(\mu_2\text{-NN})$ molecule, and this band is tentatively assigned to the N−N stretching vibration of the neutral Y_3NN complex.

We performed DFT calculations on all the possible structures, and our results show that only two structures, namely, C_s and C_{2v}, converged without imaginary frequencies, which are close in energy but very different in frequency (Figure 7). The N−N

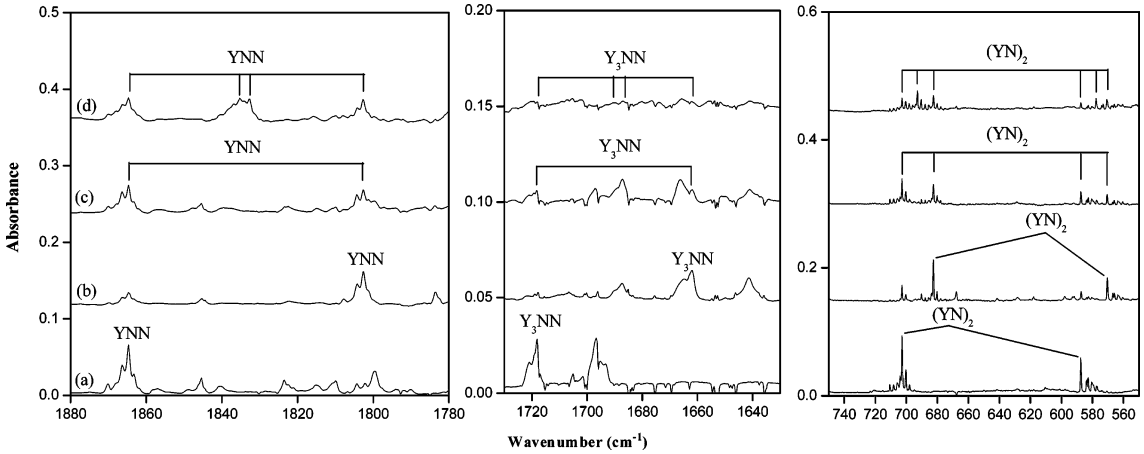

Figure 3. Infrared spectra in the 1880−1780, 1730−1630, and 750−550 cm^{-1} regions from co-deposition of laser-ablated Y atoms with N_2 and 15 mJ/pulse laser power in argon after annealing to 35 K: (a) 0.05% $^{14}N_2$; (b) 0.05% $^{15}N_2$; (c) 0.05% $^{14}N_2$ + 0.05% $^{15}N_2$; and (d) 0.05% $^{14}N_2$ + 0.1% ^{14}N ^{15}N + 0.05% $^{15}N_2$.

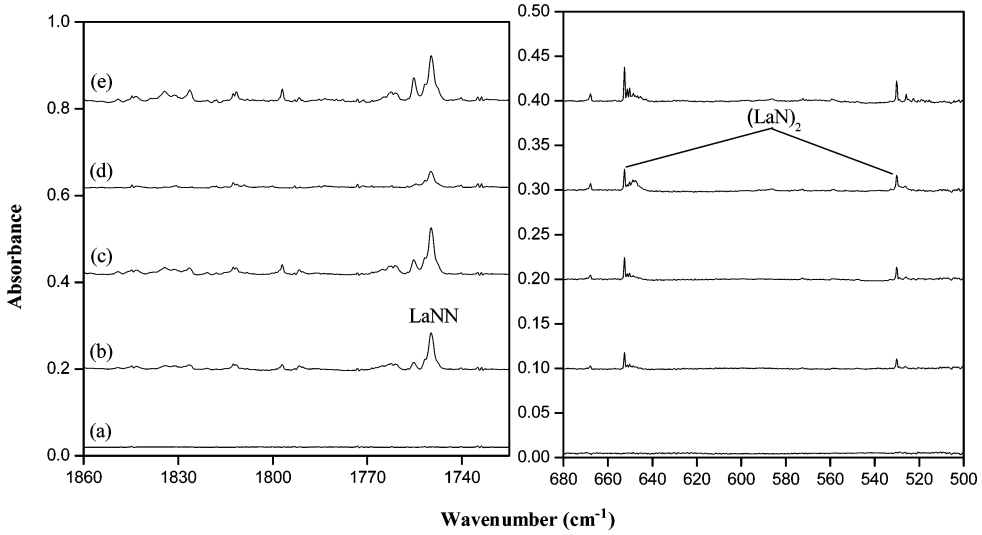

Figure 4. Infrared spectra in the 1860−1725 and 680−500 cm^{-1} regions from co-deposition of laser-ablated La atoms with 0.05% N_2 and 15 mJ/pulse laser power in argon: (a) 45 min sample deposition at 4 K; (b) after annealing to 25 K; (c) after annealing to 30 K; (d) after 12 min of broad-band irradiation; and (e) after annealing to 35 K.

stretching vibrational frequency of the C_{2v} structure is calculated at 1684.4 cm^{-1} (Tables 2 and 3), which is in accord with our observed value. As listed in Table 2, the calculated $^{14}N/^{15}N$ isotopic frequency ratio (1.0350) also is consistent with the experimental observation (1.0338). All possible structures of Y_2NN have been calculated. According to our DFT calculations, the converged μ_2-bridging geometry of the $Y_2(\mu_2\text{-NN})$ molecule is predicted to have a $^2B_1$ state with C_{2v} symmetry, which has an imaginary frequency, indicating that it is a transition state. The assignment of the Y_3NN molecule is supported by the agreement between the experimental and the calculated vibrational frequencies and isotopic shifts.

LaNN. For the experiments of laser-ablated La atoms with N_2, the absorption at 1749.8 cm^{-1} with a trapping site at 1755.3 cm^{-1} appears on annealing to 25 K, increases on annealing to 30 K, markedly decreases on broad-band irradiation, and recovers on further annealing to 35 K (Figure 4). It shifts to 1692.2 cm^{-1} with $^{15}N_2$, giving an isotopic $^{14}N/^{15}N$ ratio of 1.0340, which is characteristic of a N−N stretching vibration. No intermediate absorptions are observed in the mixed $^{14}N_2 + ^{15}N_2$ experiments, indicating that only one N_2 subunit is involved in this mode (Figure 6). In the experiment with 0.05% $^{14}N_2$ + 0.1% $^{14}N^{15}N$ + 0.05% $^{15}N_2$, four absorptions at 1749.7, 1723.1, 1719.2, and 1692.2 cm^{-1} with approximately 1:1:1:1 relative intensities are produced (Figure 6), which implies that the two N atoms are nonequivalent. As shown in Figure 5, the absorption at 1749.8 cm^{-1} dominates the spectrum in the 1920−1700 cm^{-1} region in the experiments with different N_2 concentrations and laser powers, indicating that this band is due to an initial product. Doping with CCl_4 has no effect on the band, which suggests that the product is neutral. Accordingly, this band is assigned to the N−N stretching vibration of the neutral LaNN complex, and the assignment is supported by DFT calculations (vide infra). The present observation is in disagreement with the previous report, in which a weak band at 1889.3 cm^{-1} was tentatively assigned to the LaNN molecule.[11a]

LaNN is predicted to have a $^4\Sigma^+$ ground state with a linear geometry, which lies 1.3 kcal/mol lower in energy than the La-(N_2) isomer (Figure 7). The N−N stretching vibrational frequency of LaNN is calculated at 1762.4 cm^{-1} (Tables 2 and 3), which is in accord with our observed value. As listed in Table 2, the calculated $^{14}N/^{15}N$ isotopic frequency ratio (1.0350) also is consistent with the experimental observation (1.0340). The assignment of the LaNN molecule is supported by the agreement between the experimental and the calculated vibrational frequencies and isotopic shifts.

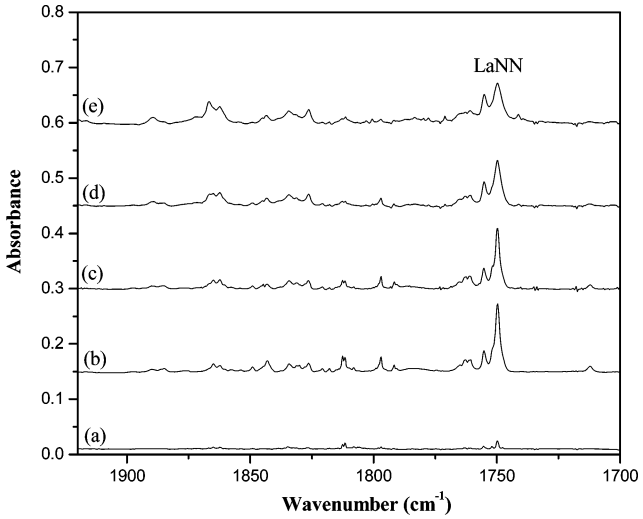

Figure 5. Infrared spectra in the 1920−1700 cm^{-1} region from co-deposition of laser-ablated La atoms with different N_2 concentrations and different laser powers after annealing to 30 K in argon: (a) 0.05% N_2 and 5 mJ/pulse; (b) 0.05% N_2 and 8 mJ/pulse; (c) 0.05% N_2 and 15 mJ/pulse; (d) 0.2% N_2 and 15 mJ/pulse; and (e) 0.5% N_2 and 15 mJ/pulse.

$(LaN)_2$. For the experiments of laser-ablated La atoms with N_2, the absorptions at 652.6 and 530.1 cm^{-1} appear on sample annealing to 25 K, visibly increase on annealing to 30 K, slightly decrease on broad-band irradiation, and markedly increase on annealing to 35 K (Figure 4). The two bands, respectively, shift to 632.9 and 513.9 cm^{-1} with $^{15}N_2$, giving isotopic frequency ratios ($^{14}N/^{15}N$, 1.0311 and 1.0315) characteristic of M−N stretching vibrations. No intermediate absorptions are observed in the mixed $^{14}N_2 + ^{15}N_2$ experiments, indicating that only two N atoms are involved in this mode (Figure 6). In the experiment with 0.05% $^{14}N_2$ + 0.1% $^{14}N^{15}N$ + 0.05% $^{15}N_2$, two sets of triplet bands (Table 1 and Figure 6) are produced, which indicates that two equivalent N atoms are involved. Doping with CCl_4 has no effect on the two bands, which suggests that the

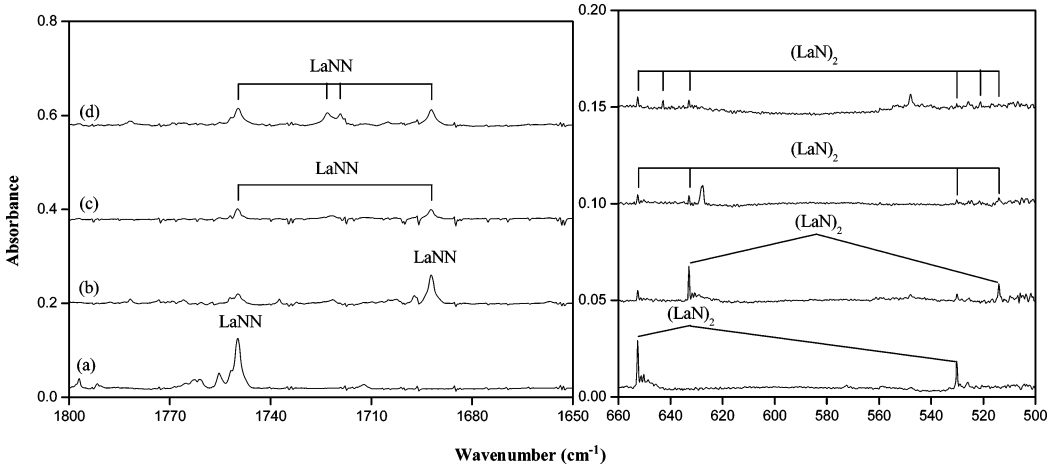

Figure 6. Infrared spectra in the 1800−1650 and 660−500 cm^{-1} regions from co-deposition of laser-ablated La atoms with N_2 and 15 mJ/pulse laser power in argon after annealing to 30 K: (a) 0.05% $^{14}N_2$; (b) 0.05% $^{15}N_2$; (c) 0.05% $^{14}N_2$ + 0.05% $^{15}N_2$; and (d) 0.05% $^{14}N_2$ + 0.1% ^{14}N ^{15}N + 0.05% $^{15}N_2$.

TABLE 3: Ground Electronic States, Point Groups, Vibrational Frequencies (cm^{-1}), and Intensities (km/mol) of Reaction Products and Isomers Calculated at the BP86/6-311++G(d,p)-SDD Level

species	electronic state	point group	frequency (intensity, mode)
YNN	$^4\Sigma^+$	C_v	1814.7 (939, Σ), 371.1 (10, Σ), 262.3 (6, π), 262.3 (6, π)
$Y(N_2)$	$^4B_1$	C_{2v}	1679.9 (668, A_1), 346.0 (20, B_2), 333.2 (2, A_1)
$(YN)_2$	^1A_g	D_{2h}	711.2 (203, b_{1u}), 653.7 (0, A_g), 557.7 (134, b_{2u}), 454.5 (0, b_{3g}), 303.3 (0, A_g), 225.5 (82, b_{3u})
Y_3NN	$^2B_1$	C_{2v}	1684.4 (497, A_1), 268.3 (2,A_1), 258.3 (5, B_1), 216.7 (2, B_2), 197.1 (1, A_1)
LaNN	$^4\Sigma^+$	C_v	1762.4 (987, Σ), 335.1 (10, Σ), 272.9 (8, π), 272.8 (8, π)
$La(N_2)$	$^4B_1$	C_{2v}	1646.5 (542, A_1), 333.1 (24, B_2), 297.3 (3, A_1)
$(LaN)_2$	^1A_g	D_{2h}	668.9 (335, b_{1u}), 621.2 (0, A_g), 532.0 (229, b_{2u}), 309.2 (0, b_{3g}), 245.9 (0, A_g), 229.4 (83, b_{3u})

product is neutral. The two bands are assigned to the La−N stretching vibrations of the neutral $(LaN)_2$ complex, which is in agreement with the previous assignment in solid argon (652.3 and 529.9 cm^{-1}).[11a]

The present DFT calculations lend strong support for the assignment of $(LaN)_2$. Similar to the $(ScN)_2$ and $(YN)_2$ molecules,[11c] the $(LaN)_2$ molecule is predicted to have a ^1A_g ground state with D_{2h} symmetry (Figure 7), which is 33.7 and 90.3 kcal/mol lower in energy than the triplet and quintet ones, respectively. In contrast to the previous reports,[11a,c] the present DFT calculations predict that $(LaN)_2$ has b_{1u} and b_{2u} La−N stretching vibrational frequencies at 668.9 and 532.0 cm^{-1} (Tables 2 and 3), which are in accord with our observed values (652.6 and 530.1 cm^{-1}). As listed in Table 2, the calculated $^{14}N/^{15}N$ isotopic frequency ratios (1.0316 and 1.0316) also are consistent with the experimental observations (1.0311 and 1.0315). According to our DFT calculations, the b_{3u} mode frequency (229.4 cm^{-1}) of $(LaN)_2$ is too low to be observed in the present experiment (Table 3). The assignment of the $(LaN)_2$ molecule is supported by the agreement between the experimental and the calculated vibrational frequencies and isotopic shifts.

Other Absorptions. As compared to the previous experiments using large N_2 concentrations,[11a] new absorptions at 1845.5, 1823.4, and 1799.6 cm^{-1} are observed in the present experiments of laser-ablated Y atoms with N_2. These bands may be due to the N−N stretching vibrations of the $(NN)_xY(NN)$ species (Table 1). In the present experiments of laser-ablated La atoms with N_2, new absorptions at 1826.4, 1797.0, and 1791.6 cm^{-1} may be due to the N−N stretching vibrations of the $(NN)_xLaNN$ species (Table 1).

Reaction Mechanism. In our experiments, no any nitride absorptions were observed in the as-deposited and annealed spectra, suggesting that in the present experiments, the laser ablation conditions were not violent enough for generating Y and La atoms with high energies to cause the dissociation of molecular nitrogen to generate N atoms,[18,19] indicating that the observed products were formed by low-temperature reactions of the metal atoms with molecular N_2. On the basis of the behavior observed in the experiment, plausible reaction mechanisms can be proposed as follows. Laser-ablated Y atoms are co-deposited with N_2 to form the YNN, $(YN)_2$, and Y_3NN complexes (Figure 1). The species increase on annealing, suggesting that the ground state Y atoms can react with N_2 molecules to form YNN, $(YN)_2$, and Y_3NN complexes spontaneously according to reactions 1−4, which are predicted to be exothermic. The formation mechanisms of $(MN)_2$ molecules (M = Sc, Ti, and Gd) have been discussed in detail recently.[9d−e] Similarly, the reaction of Y_2 ($^5\Sigma_u^-$) with N_2 may proceed via two intermediates to form the rhombic $Y(\mu_2\text{-}N)_2Y$ molecule, as shown in Figure 8. The formation of the $Y_2(\mu\text{-}\eta^1\text{:}\eta^2\text{-}N_2)$ intermediate with a planar C_s structure (Figure 7) is the initial step, which is predicted to be exothermic by 47 kcal/mol from the ground state Y_2 ($^5\Sigma_u^-$) and N_2. The N−N bond dissociation reaction $(Y_2(\mu\text{-}\eta^1\text{:}\eta^2\text{-}N_2) \rightarrow Y(\mu_2\text{-}N)_2Y)$ is predicted to be exothermic by 42 kcal/mol and proceeds via a nonplanar bridge-bonded C_{2v} intermediate $Y_2[\eta^2\text{-}(\mu_2\text{-}N)_2]$ (Figure 7), which lies 11 kcal/mol lower in energy than the $Y_2-(\mu\text{-}\eta^1\text{:}\eta^2\text{-}N_2)$ intermediate

$$Y\ (^2D) + N_2 \rightarrow YNN\ (^4\Sigma^+) \quad \Delta E = -12.0\ \text{kcal/mol} \qquad (1)$$

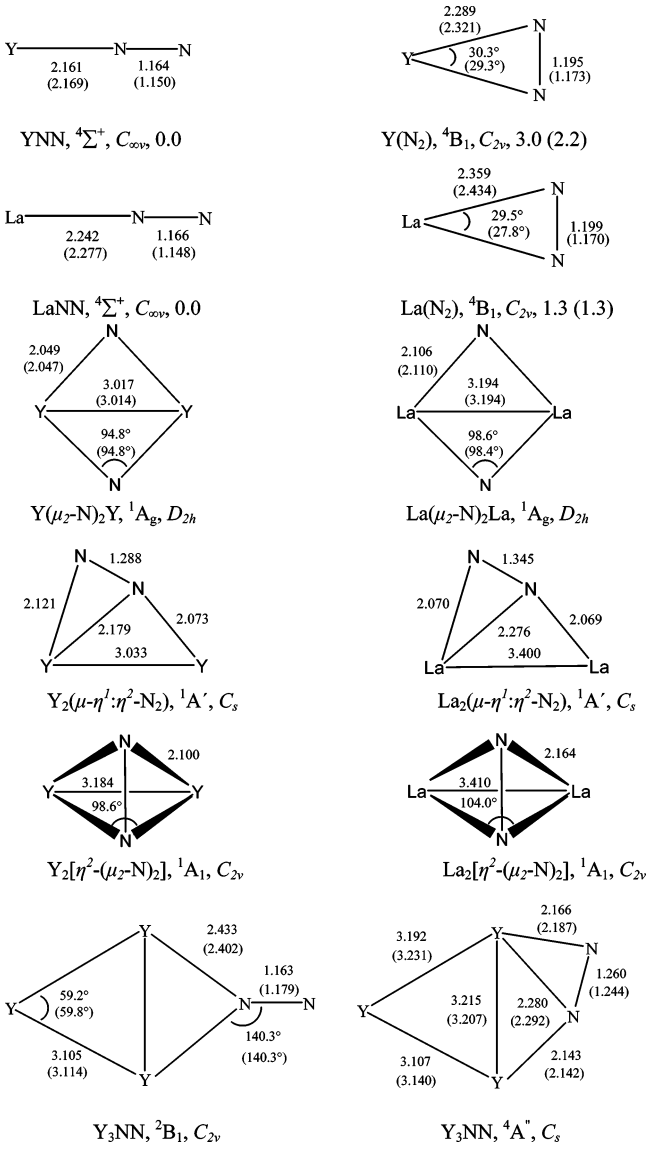

Figure 7. Optimized structures (bond length in angstroms and bond angles in degrees), electronic ground states, point groups, and relative energies (in kilocalories per mole) of the possible products, intermediates, and isomers calculated at the BP86/6-311++G(d,p)-SDD and B3LYP/6-311++G(d,p)-SDD (in parentheses) levels.

$$Y\ (^2D) + Y(^2D) \rightarrow Y_2\ (^5\Sigma_u^-) \quad \Delta E = -34.5\ \text{kcal/mol} \qquad (2)$$

$$Y_2\ (^5\Sigma_u^-) + N_2 \rightarrow (YN)_2\ (^1A_g) \quad \Delta E = -89.2\ \text{kcal/mol} \qquad (3)$$

$$3Y\ (^2D) + N_2 \rightarrow Y_3NN\ (^2B_1) \quad \Delta E = -102.1\ \text{kcal/mol} \qquad (4)$$

Under the present experimental conditions, laser-ablated La atoms are co-deposited with N_2 to form the LaNN and $(LaN)_2$ complexes on annealing to 25 K (Figure 4), which markedly increase on further annealing, suggesting that the ground state La atom can react with the N_2 molecule to form the LaNN and $(LaN)_2$ complexes spontaneously according to reactions 5−7, which are predicted to be exothermic. As shown in Figure 8, the reaction of La_2 ($^5\Sigma_u^-$) with N_2 to form the rhombic La(μ_2-N)$_2$La molecule proceeds via two intermediates (Figure 7). The formation of the La$_2$−(μ-η^1:η^2-N$_2$) intermediate with a planar C_s structure is the initial step, which is predicted to be exothermic by 57 kcal/mol from the ground state La_2 ($^5\Sigma_u^-$) and N_2. The N−N bond dissociation reaction (La$_2$−(μ-η^1:η^2-N$_2$) → La(μ_2-N)$_2$La) is exothermic by 62 kcal/mol and proceeds

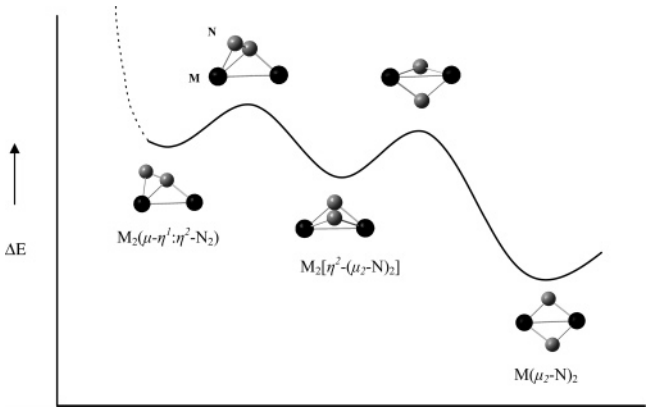

Figure 8. Schematic potential energy profile for $M_2 + N_2 \rightarrow M(\mu_2\text{-}N)_2M$ (M = Y or La). The dashed line indicates the computationally unexplored spin-crossing area.

via a nonplanar bridge-bonded C_{2v} intermediate La$_2$[η^2-(μ_2-N)$_2$], which lies 14 kcal/mol lower in energy than the La$_2$−(μ-η^1:η^2-N$_2$) intermediate

$$La\ (^2D) + N_2 \rightarrow LaNN\ (^4\Sigma^+) \quad \Delta E = -75.3\ \text{kcal/mol} \qquad (5)$$

$$La\ (^2D) + La\ (^2D) \rightarrow La_2\ (^5\Sigma_u^-) \quad \Delta E = -163.3\ \text{kcal/mol} \qquad (6)$$

$$La_2\ (^5\Sigma_u^-) + N_2 \rightarrow (LaN)_2\ (^1A_g) \quad \Delta E = -119.3\ \text{kcal/mol} \qquad (7)$$

Conclusion

Yttrium and lanthanum nitrides and dinitrogen complexes (YNN, $(YN)_2$, Y_3NN, LaNN, and $(LaN)_2$) were prepared by the reactions of laser-ablated yttrium and lanthanum atoms with N_2 in excess argon. On the basis of the isotopic shifts and splitting patterns, the molecules (YNN, $(YN)_2$, Y_3NN, LaNN, and $(LaN)_2$) were characterized. DFT calculations were performed, which lend support to the experimental assignments of the infrared spectra. The ground-state yttrium and lanthanum atoms reacted with N_2 to form YNN, $(YN)_2$, Y_3NN, LaNN, and $(LaN)_2$ complexes spontaneously upon annealing.

Acknowledgment. The authors thank the reviewers for valuable suggestions and comments. This work was supported by a Grant-in-Aid for Scientific Research (B) (Grant 17350012) from the Ministry of Education, Culture, Sports, Science and Technology (MEXT) of Japan. Y.-L.T. thanks JASSO and Kobe University for an Honors Scholarship.

References and Notes

(1) Howard, J. B.; Rees, D. C. *Chem. Rev.* **1996**, *96*, 2965.
(2) Burgess, N. K.; Lowe, D. J. *Chem. Rev.* **1996**, *96*, 2983.
(3) Pool, J. A.; Lobkovsky, E.; Chirik, P. J. *Nature (London, U.K.)* **2004**, *427*, 527.
(4) Allen, A. D.; Senoff, C. V. *Chem. Commun. (Cambridge, U.K.)* **1965**, 621.
(5) (a) Fryzuk, M. D.; Johnson, S. A. *Coord. Chem. Rev.* **2000**, *200*, 379. (b) Richards, R. L. *Coord. Chem. Rev.* **1996**, *154*, 83.
(6) Hidai, M.; Mizobe, Y. *Chem. Rev.* **1995**, *95*, 1115.
(7) (a) Blomberg, M. R. A.; Siegbahn, P. E. M. *J. Am. Chem. Soc.* **1993**, *115*, 6908. (b) Kardahakis, S.; Koukounas, C.; Mavridis, A. *J. Chem. Phys.* **2006**, *124*, 104306. (c) Berces, A.; Mitchell, S. A.; Zgierski, M. Z. *J. Phys. Chem. A* **1998**, *102*, 6340.
(8) Siegbahn, P. E. M.; Blomberg, M. R. A. *Chem. Rev.* **2000**, *100*, 421.
(9) (a) Zhou, M. F.; Zhang, L.; Qin, Q. Z. *J. Phys. Chem. A* **2001**, *105*, 6407. (b) Zhou, M. F.; Wang, G. J.; Zhao, Y. Y.; Chen, M. H.; Ding, C .F. *J. Phys. Chem. A* **2005**, *109*, 5079. (c) Zhou, M. F.; Jin, X.; Li, J.

Angew. Chem., Int. Ed. **2007**, *46*, 2911. (d) Gong, Y.; Zhao, Y. Y.; Zhou, M. F. *J. Phys. Chem. A* **2007**, *111*, 6204. (e) Himmel, H. J.; Hübner, O.; Klopper, W.; Manceron, L. *Angew. Chem., Int. Ed.* **2006**, *45*, 2799.

(10) Chen, M. H.; Wang, G. J.; Zhou, M. F. *Chem. Phys. Lett*. **1998**, *409*, 70.

(11) (a) Chertihin, G. V.; Bare, W. D.; Andrews, L. *J. Phys. Chem. A* **1998**, *102*, 3697. (b) Willson, S. P.; Andrews, L. *J. Phys. Chem. A* **1998**, *102*, 10238. (c) Chertihin, G.; Andrews, L.; Bauschlicher, C. W., Jr. *J. Am. Chem. Soc.* **1998**, *120*, 3205. (d) Willson, S. P.; Andrews, L. *J. Phys. Chem. A* **1999**, *103*, 1311. (e) Andrews, L.; George, V. A. C.; William, D. B.; Neurock, M. *J. Phys. Chem. A* **1998**, *102*, 2561.

(12) Zhou, M. F.; Andrews, L.; Bauschlicher, C. W., Jr. *Chem. Rev*. **2001**, *101*, 1931.

(13) (a) Burkholder, T. R.; Andrews, L. *J. Chem. Phys*. **1991**, *95*, 8697. (b) Zhou, M. F.; Tsumori, N.; Andrews, L.; Xu, Q. *J. Phys. Chem. A* **2003**, *107*, 2458. (c) Jiang, L.; Xu, Q. *J. Chem. Phys.* **2005**, *122*, 34505.

(14) Frisch, M. J.; Trucks, G. W.; Schlegel, H. B.; Scuseria, G. E.; Robb, M. A.; Cheeseman, J. R.; Montgomery, J. A., Jr.; Vreven, T.; Kudin, K. N.; Burant, J. C.; Millam, J. M.; Iyengar, S. S.; Tomasi, J.; Barone, V.; Mennucci, B.; Cossi, M.; Scalmani, G.; Rega, N.; Petersson, G. A.; Nakatsuji, H.; Hada, M.; Ehara, M.; Toyota, K.; Fukuda, R.; Hasegawa, J.; Ishida, M.; Nakajima, T.; Honda, Y.; Kitao, O.; Nakai, H.; Klene, M.; Li, X.; Knox, J. E.; Hratchian, H. P.; Cross, J. B.; Adamo, C.; Jaramillo, J.; Gomperts, R.; Stratmann, R. E.; Yazyev, O.; Austin, A. J.; Cammi, R.; Pomelli, C.; Ochterski, J. W.; Ayala, P. Y.; Morokuma, K.; Voth, G. A.; Salvador, P.; Dannenberg, J. J.; Zakrzewski, V. G.; Dapprich, S.; Daniels, A. D.; Strain, M. C.; Farkas, O.; Malick, D. K.; Rabuck, A. D.; Raghavachari, K.; Foresman, J. B.; Ortiz, J. V.; Cui, Q.; Baboul, A. G.; Clifford, S.; Cioslowski, J.; Stefanov, B. B.; Liu, G.; Liashenko, A.; Piskorz, P.; Komaromi, I.; Martin, R. L.; Fox, D. J.; Keith, T.; Al-Laham, M. A.; Peng, C. Y.; Nanayakkara, A.; Challacombe, M.; Gill, P. M. W.; Johnson, B.; Chen, W.; Wong, M. W.; Gonzalez, C.; Pople, J. A. *Gaussian 03*, revision B.04; Gaussian, Inc.: Pittsburgh, PA, 2003.

(15) (a) Becke, A. D. *Phys. Rev. A: At., Mol., Opt. Phys*. **1988**, *38*, 3098. (b) Perdew, J. P. *Phys. Rev. B: Condens. Matter Mater. Phys*. **1986**, *33*, 8822. (c) Lee, C.; Yang, E.; Parr, R. G. *Phys. Rev. B: Condens. Matter Mater. Phys.* **1988**, *37*, 785. (d) Becke, A. D. *J. Chem. Phys*. **1993**, *98*, 5648.

(16) (a) Krishnan, R.; Binkley, J. S.; Seeger, R.; Pople, J. A. *J. Chem. Phys*. **1980**, *72*, 650. (b) Frisch, M. J.; Pople, J. A.; Binkley, J. S. *J. Chem. Phys*. **1984**, *80*, 3265.

(17) Dolg, M.; Stoll, H.; Preuss, H. *J. Chem. Phys*. **1989**, *90*, 1730.

(18) Kang, H.; Beauchamp, J. L. *J. Phys. Chem.* **1985**, *89*, 3364.

(19) Thiem, T. L.; Salter, R. H.; Gardner, J. A. *Chem. Phys. Lett*. **1994**, *218*, 309.